Engineering Symposium at Bánki
(ESB 2024)

Predicting Anterior Cruciate Ligament Changes During Unexpected Side Cutting Based on Inertial Sensors

[1]Enze Shao, [2] Tibor Goda

[1] *Obuda University. Doctoral School on Safety and Security Sciences, Budapest, Hungary, shaoenze@hotmail.com*
[2] *Obuda University. Doctoral School on Safety and Security Sciences, Budapest, Hungary, goda.tibor@bgk.uni-obuda.hu*

Abstract

In sports and athletic competitions, efficient lateral cutting maneuvers (LCMs) and directional changes are essential for optimal performance. This study involved 18 male athletes who were screened by professional physicians. A Random Forest classification model was employed to predict anterior cruciate ligament (ACL) injuries during outdoor LCMs and running. Results indicated that during 90° LCMs, compared to LCMs in other directions and running, the knee joint experienced greater flexion angles, increased abduction moments, and elevated coronal-plane knee contact forces. OpenSim calculations further demonstrated significantly higher ACL strain values during 90° LCMs relative to other movement conditions. Training and validation of inertial sensor data using the Random Forest model revealed high sensitivity and accuracy in identifying key time-domain and frequency-domain features, specifically "kurtosis," "skewness," "variance," "energy," and the "25th percentile."

Keywords: Lower limb biomechanics, anterior cruciate ligament, inertial sensors, machine learning

1. Introduction

In the aftermath of the COVID-19 pandemic, promoting physical and mental health through exercise has garnered widespread attention. With the implementation of relevant policies, participation in sports such as basketball, football, and badminton in stadiums has become increasingly accessible. In these sports, the ability to perform rapid directional changes and lateral cutting maneuvers (LCMs) is crucial for success [1]. Consequently, optimizing LCM execution for individuals and teams plays a significant role in both training and competition [2].

Successful execution of LCMs relies on two key requirements [3]. First, the center of mass (COM) must decelerate in the original direction and accelerate toward the new direction of motion. Second, the body must rotate accordingly toward the new direction. Research indicates that during 90° LCMs, the final ground contact before the transition phase is responsible for most deceleration. In contrast, the transition phase primarily facilitates acceleration into the new direction [4].

To achieve COM deceleration, athletes must produce a backward-directed ground reaction force (GRF) by positioning their COM behind the center of force application (CFA). Conversely, to accelerate in the new direction, they need to generate a forward-directed GRF by positioning their COM ahead of the CFA. Efficient transition between deceleration and acceleration within a short time frame is a key determinant of high-performance LCMs.

Research indicates that 72% of ACL injuries result from non-contact mechanisms, while 28%

are caused by contact mechanisms [5]. A common non-contact mechanism involves deceleration before or during directional changes [6]. Building on these findings, numerous studies have examined lateral cutting maneuvers (LCMs) [7], landings [8], and jumping tasks [9], identifying harmful lower extremity biomechanics, such as increased knee valgus moments, elevated quadriceps EMG activity, and greater knee valgus angles—all associated with non-contact anterior cruciate ligament (ACL) injuries.

Traditional assessments of lower extremity injuries rely on 3D motion analysis systems and force plates to capture kinematic and kinetic data [10]. However, these methods are costly and spatially restrictive, limiting their use in clinical and sports settings [11,12]. In contrast, wearable devices can capture athletes' biomechanical characteristics in real-world environments, offering valuable insights for on-site analysis of complex movements [13,14]. Inertial Measurement Units (IMUs)—which integrate gyroscopes, accelerometers, and magnetometers—are the leading tools for quantifying movement behaviors [15].

Studies combining inertial sensors with machine learning have demonstrated the effectiveness of these tools in preventing sports injuries [16-18]. Researchers collect data on post-surgery characteristics, technical errors in patients or athletes, and movement patterns of healthy individuals. After data post-processing and action recognition, these datasets are used to train algorithmic models. For injury prevention or rehabilitation diagnostics, classification models with binary outputs ("0" or "1") are typically employed to indicate correct or incorrect movements, or injury presence or absence. These labeled inputs and outputs provide a clear and practical basis for decision-making in research and clinical practice.

Building on these promising results, ACL injury prevention research can adopt a similar approach. Collecting movement characteristics associated with elevated ACL loads and comparing them to those with normal ACL loads, a machine learning classification model can be applied to distinguish between these conditions. This method may enhance the assessment of ACL injury risk during lateral cutting maneuvers (LCMs).

2. Methods

2.1 Participant Recruitment

A total of 25 healthy male university students from Ningbo, who regularly engaged in sports involving frequent side-cutting movements (such as basketball, football, and frisbee) at least three times per week, were recruited through offline promotions, online recruitment, and other methods. All participants were free of foot deformities, lower limb muscle or joint injuries, and had no history of sports-related injuries or surgeries within the six months before the experiment. The experimental process and requirements were clearly explained to participants beforehand.

To ensure eligibility, all participants underwent magnetic resonance imaging (MRI) scans and were assessed by professional physicians for knee ligament integrity. Ultimately, 18 participants met the minimum sample size criteria and were included in the study. All participants demonstrated right-leg dominance.

The study was approved by the Ethics Committee of the Ningbo University Research Institute (RAGH20220929, September 29, 2022). Written informed consent was obtained from all participants, who were made aware of the study's objectives, procedures, and requirements.

2.2 Experimental Procedure

The Delsys EMG system (Delsys, Boston, MA, USA) was used to synchronously collect EMG signals from the right leg's biceps femoris, rectus femoris, tibialis anterior, and gastrocnemius muscles at a sampling frequency of 1000 Hz for validation in the OpenSim model [19]. Infrared photoelectric timers (Smart Speed, Fusion Sport Inc., Burbank, CA, USA) monitored lateral cutting maneuver (LCM) speeds and calculated participants' maximum sprint speeds. Inertial sensors (IMeasureU V1, Auckland, New Zealand; dimensions: 40 × 28 × 15 mm, weight: 12g, resolution: 16 bit) were affixed to the proximal and distal anteromedial tibiae of each participant's dominant leg using elastic bands, aligned with the vertical axis of the tibiae (see Figure 1) [20].

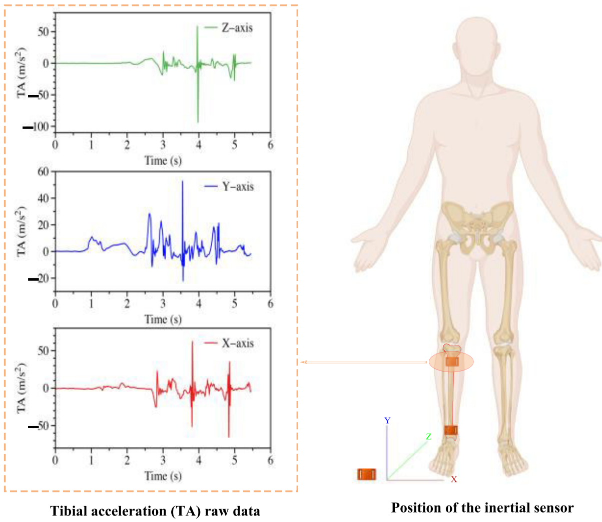

Figure 1. Raw tibial acceleration data (left) and anatomically fixed position of the IMU (right)

Participants wore standardized tight shorts and identical footwear during testing. Each session began with a 10-minute warm-up guided by a professional fitness coach. Eligible male athletes performed LCM tests in a laboratory setting.

Before the LCM test, participants completed three static standing trials by standing with feet shoulder-width apart on a force plate. For the LCM biomechanical tests and IMU data collection, participants accelerated to 70% of their previously measured maximum sprint speed upon the experimenter's command. After a 10-meter sprint, they entered the designated change-of-direction area (approximately 2 meters from the force plate) and executed LCMs or running actions according to randomly illuminated lights.

Prior to each trial, participants stood still for 3 seconds at the starting position to facilitate the segmentation of acceleration phases, gyroscope data acquisition, and movement direction correction. The random light sequence was limited to a maximum of two repetitions to minimize the impact of familiarity on coordination and reaction speed.

2.3 Data Processing

Three-dimensional knee joint models were generated for all participants from MRI scans and analyzed following virtual ACL reconstruction using finite element software. Image segmentation to define skeletal boundaries was performed using Mimics 20.0 (Materialise, Leuven, Belgium). To refine uneven surfaces caused by stacked medical images, Geomagic Studio 2013 (Geomagic, Inc., Research Triangle Park, NC, USA) was employed. Each processed surface component was then imported into SolidWorks 2020 (SolidWorks Corporation, MA, USA) to create solid parts. In SolidWorks 2020, ligaments and muscle tissues were reconstructed based on the anatomical characteristics of the knee and ankle joints.

Previous studies have shown that the ACL exhibits viscoelastic properties, with tensile behavior dependent on strain rate or loading rate [21]. Consequently, the ACL was modeled as a nonlinear elastic passive soft tissue [22], with fixed insertion points in the femur and tibia.MATLAB was used for coordinate system conversion, low-pass filtering, data extraction, and dataset format conversion [19]. Kinematic data for static calibration and joint angle calculations were obtained from ".trc" files, while kinetic data, such as ground reaction forces, centers of pressure, and torques, were contained in ".mot" files. Marker trajectories from LCM trials were processed using OpenSim 4.2 (Stanford University, Stanford, CA, USA) to derive kinematic and kinetic data of the participants.

Tibial accelerations during LCMs were synchronously recorded with a triaxial accelerometer at a frequency of 500 Hz, both in laboratory and field conditions. Linear trends in the raw data were removed using the least-squares best-fit line method [23]. A second-order Butterworth low-pass filter with a 60 Hz cut-off frequency was then applied [24]. While axial acceleration is frequently reported, recent studies advocate for the assessment of resultant acceleration [25,26]. Therefore, this study calculated resultant acceleration (RA) using the following formula:

$$\mathrm{RA}= \sqrt{x^2 + y^2 + z^2}$$

2.4 Establishment, Training, and Validation of the Random Forest Machine Learning Model

In this study, six types of data features were extracted from two IMUs, with each IMU transmitting three-axis data features. Given the highly nonlinear and continuous nature of these input variables, the random forest method was deemed appropriate for analysis [27].

A robust nonlinear classifier, the random forest, was used to develop the classification model, comprising 128 decision trees. This number was determined after evaluating the accuracy of tree quantities ranging from 1 to 500. Although classification accuracy generally improves with more trees, gains beyond 128 trees were negligible.

To balance the training data for binary classification (i.e., acceptable vs. abnormal repetitions), random instances from the overrepresented category were removed. Participants were excluded from analysis if they did not perform at least two repetitions per classification category, as insufficient data would hinder model training and testing.

Model performance was evaluated using accuracy, sensitivity, and specificity metrics. Accuracy represents the overall classifier effectiveness and is calculated as the ratio of correctly classified examples to the total number of examples. Sensitivity measures the classifier's ability to identify the target label, while specificity assesses its ability to detect the negative label.

$$Accuracy = \frac{TP + TN}{TP + FP + TN + FN}$$

$$Sensitivity = \frac{TP}{TP + FN}$$

$$Specificity = \frac{TN}{TN + FP}$$

2.5 Statistical Analysing

All statistical analyses were conducted using SPSS 26.0 (IBM, NY, USA) and MATLAB R2018a (The MathWorks, Natick, MA, USA). The Shapiro-Wilk test was performed to assess

Gaussian normality. For data that did not meet normality assumptions, a secondary check was conducted using the Q-Q normal distribution plot. Based on the results of the normality tests [28], one-way repeated measures ANOVA with Statistical Parametric Mapping (SPM1d) or Non-Parametric Mapping (SnPM1d) was used to compare knee joint angles, moments, contact forces, and ACL strains across different side-cutting directions and running during the LCM phase. Holm-Bonferroni correction was applied to account for multiple comparisons. Pearson correlation coefficients (r^2) were calculated to assess linear relationships between ACL stress and strain.

Statistical Parametric Mapping (SPM) involves analyzing one-dimensional biomechanical data, such as joint angles, moments, ground reaction forces, and electromyography, after temporal-spatial smoothing and standardization. Originating from neuroimaging, SPM offers advantages over traditional methods that assess discrete points, enabling the analysis of continuous biomechanical data.

3. Methods

3.1 Kinematics

The results showed that there were significant differences in knee flexion-extension angles among subjects when performing 90°, 45° LCM, and running (5%-95% of the stance phase, $P<0.001$, $F=4.162$); there were significant differences in knee internal-external rotation angles during 8%-91% of the lower limb support phase ($P=0.001$, $F=12.615$); and there were significant differences in knee abduction-adduction angles during 0%-100% of the lower limb support phase ($P<0.001$, $F=6.452$). Post-hoc comparison of knee flexion angles revealed that knee flexion angles during 90° LCM were significantly greater than those during 45° LCM ($P<0.001$) and running ($P<0.001$), respectively, during 20%-82% and 8%-95% of the support phase; knee flexion angles during 45° LCM were significantly greater than those during running ($P<0.001$). Using one-way repeated measures ANOVA in SnPM1d, the results showed that there were significant differences in knee strain changes among subjects when performing 90°, 45° LCM, and running (0-100% of the support phase, $P<0.001$, $F=12.162$).

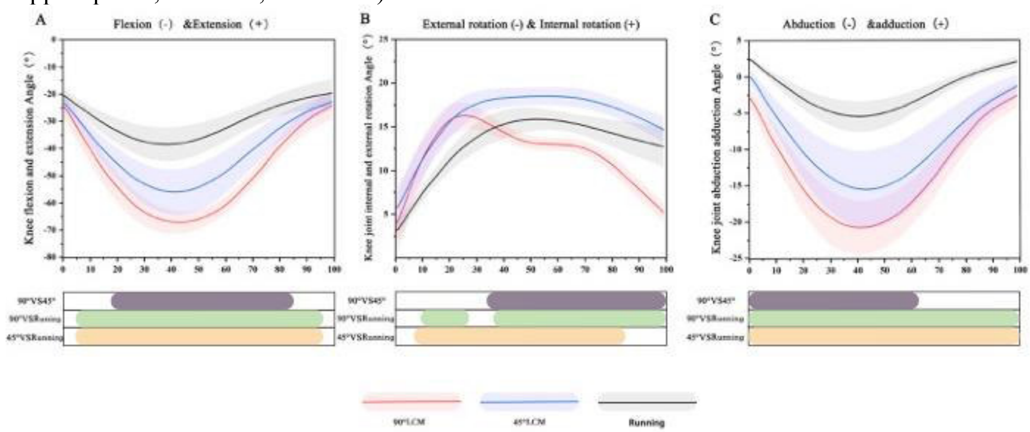

Figure 2. Changes in the joint angle of the knee joint during the support period during various movement states,

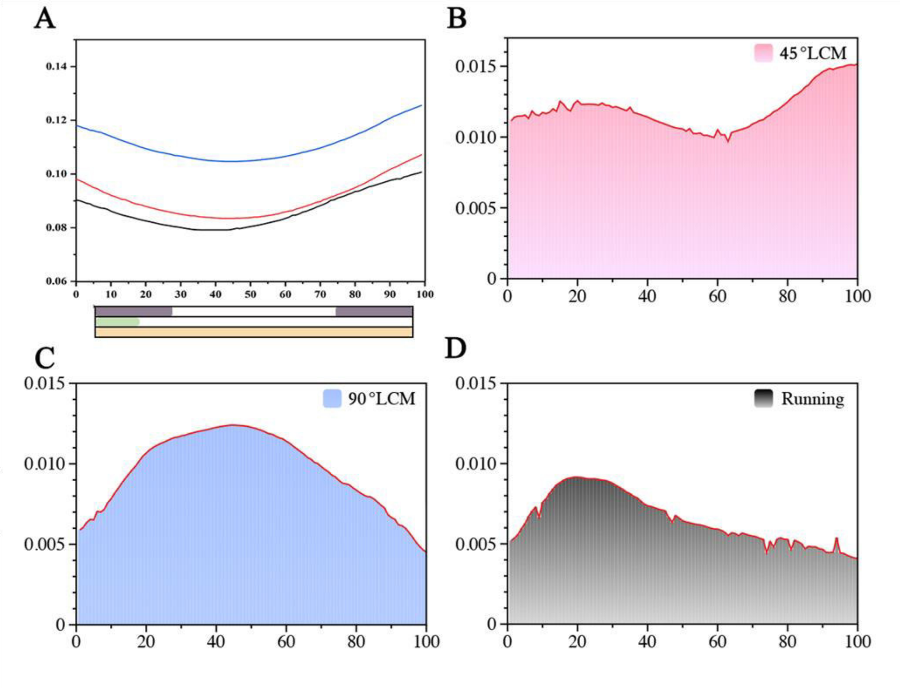

Figure 3. The ACL strain of the knee joint was changed during 45°, 90° LCM, and running. Figures B, C, and D represent the change in standard deviation at 45°, 90° LCM, and running, respectively.

3.2 Dynamics

Using the one-dimensional single-factor repeated measures ANOVA in SnPM1d, the results showed that there were statistically significant differences in knee flexion-extension moments during the 0%-45% (*P*=0.01) and 55%-98% (*P*=0.01) stance phases, as well as internal-external rotation moments during the 10%-100% (*P*=0.042) stance phase, and abduction-adduction moments during the 0%-15% (*P*=0.01) and 20%-100% (*P*=0.01) stance phases when subjects completed 90°, 45° LCM (Lateral Cut Movement), and running. Post-hoc comparisons of knee flexion-extension moments revealed that the knee flexion moment during 90° LCM was significantly smaller than that during 45° LCM in the 0%-6% and 65%-85% stance phases (*P*=0.01 and *P*=0.01, respectively) and significantly larger than that during running in the 11%-30% and 55%-72% stance phases (P=0.001 and *P*=0.001, respectively). The results of the one-dimensional single-factor repeated measures ANOVA in SnPM1d also showed that there were statistically significant differences in contact forces in the sagittal plane (10%-100%), frontal plane (10%-30%, 60%-87%), and transverse plane (10%-34%, 40%-60%) of the knee joint during 90°, 45° LCM, and running, with statistical results of *P*=0.020, *P*=0.042, and *P*=0.030, respectively. Post-hoc comparisons of sagittal plane contact forces revealed that knee contact forces during 45° LCM were significantly greater than those during 90° LCM (10%-99% stance phase, *P*<0.001) and running (20%-80% stance phase, *P*<0.001); during the 38%-80% stance phase, knee contact forces during 90° LCM were significantly greater than those during running (*P*<0.05).

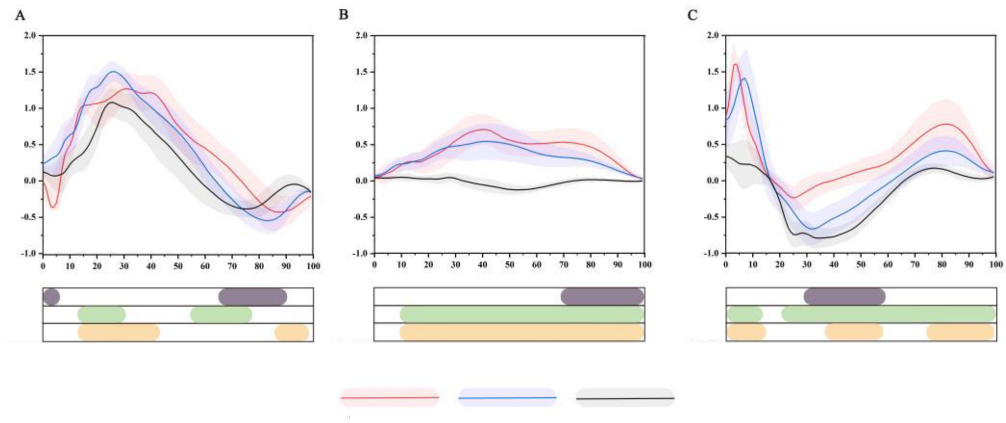

Changes in joint moments of the knee joint during the support period for various movement states

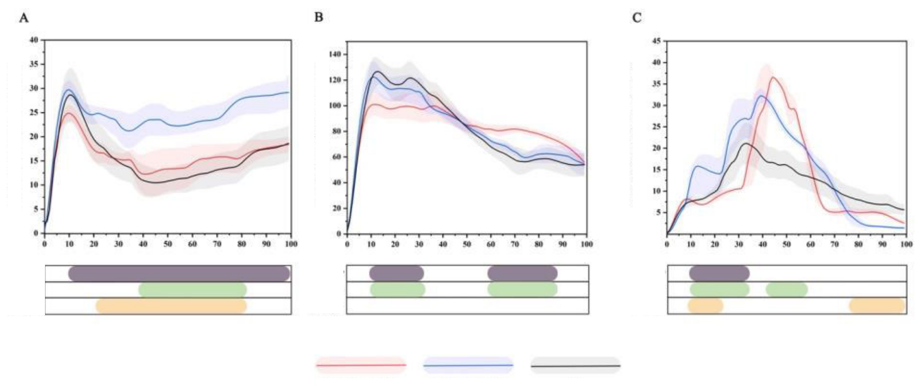

Figure 5 Variation of joint contact forces at the knee joint during the support period for various states of motion

3.3 Performance of the "Random Forest" Classification Model

In this study, a total of 18 subjects were recruited to collect 300 sets of feature data from two IMUs (Inertial Measurement Units) outdoors and indoors during 45°, 90°, 135°, 180° LCM, and running, totaling 600 sets of IMU data as the overall dataset. Among them, IMU data with ACL strain levels between 9% and 15% and accounting for more than 50% of the standing phase during a complete movement were considered as "high ACL strain IMU data," and a total of 150 sets of data were obtained through OpenSim simulation calculations, while the remaining data were considered as "low ACL strain IMU data." "Mean," "RMS" (Root Mean Square), "standard deviation," "kurtosis," "median," "skewness," "variance," "maximum value," "minimum value," "energy," "25th percentile," and "75th percentile" were used as the feature values for each set of IMU data for training and obtained the following training performance (See Table 1).

Table 1. Training results for feature data

Eigenvalue	Accuracy (%)	Sensitivity (%)	Specificity (%)
Mean value	82	80	93
RMS	85	72	90
Kurtosis	96	86	92
Mid-value	92	88	90
Skewness	97	90	86
Yariance	95	88	88
Maximum value	90	82	93
Minimum value	91	83	80
Energy	96	92	82
The 25th percentile	96	89	93
The 75th percentile	92	90	91

4. Discussion

This study employed finite element simulation software, such as Mimics and Geomagic Studio, to model nonlinear elastic passive soft tissues and imported them into the OpenSim platform to create personalized musculoskeletal models. The secondary aim was to investigate the impact of different LCM directions on lower limb biomechanics by comparing knee joint angles, moments, and contact forces during the stance phase of LCMs in various directions and running. Additionally, ACL strain and stress were quantified using the CMC (Computed Muscle Control) and FD (Force Direction) tools. The findings revealed that during rapid deceleration and direction change in 135° and 180° LCM scenarios, the early involvement of the hip joint and the forward shift of the body's center of mass resulted in significantly lower ACL strain compared to the 90° LCM, with a strain range between 9%-10%. Consequently, this study focused on LCM directions between 90° and 45°. Furthermore, the study aimed to classify and train LCM feature data from different directions by developing a machine learning classification model, with the goal of enabling accurate ACL injury assessment using a small number of portable sensors.

The results of this study indicated that the knee flexion and valgus angles during 90° LCM were significantly greater than those during 45° LCM and running. This could be because athletes need to make a more substantial change in direction during the 90° LCM, requiring the knee joint to undergo a larger range of flexion and rotation. Such movements likely place higher demands on knee joint stability and motor control, potentially increasing the risk of knee injuries. By positioning the knee closer to the resultant ground reaction force vector, frontal plane knee motion directly affects multiplanar knee loads. Previous studies have introduced the concept of the "dynamic valgus" position, where valgus knees, adducted and internally rotated hips, and valgus ankles with internal rotation are identified as established risk factors for non-contact ACL injuries. Consequently, researchers recommend that athletes align the sagittal plane of the knee joint during LCMs. Our results showed an initial varus moment at the knee, which could significantly impact ACL loading.

Previous studies have identified externally applied knee flexion moments and varus moments as major contributors to ACL stress. As the knee approaches full extension at heel strike, the ground reaction force arm increases perpendicular to the knee, thereby amplifying the anterior shear force and potentially increasing ACL loads. In other words, greater flexion moments lead to higher tibial angular acceleration, which may induce larger ACL strains. A similar theoretical framework was presented by Jones P.A. et al., who confirmed a significant negative correlation between side trunk inclination and flexion moments. However, the methodological quality of that study was low (33% of the expected standard), and the correlation between trunk muscle activation and knee abduction moments, as mentioned above, prevents it from being the sole basis for conclusions.

IMUs bridge the gap between laboratory and clinical biomechanical assessments, enabling the acquisition of objective human motion data in unconstrained environments at a low cost. This capability has led to further research and discussions. Combining machine learning and IMUs for classifying or predicting known datasets is currently a cost-effective and applicable method. Studies have demonstrated that IMU systems can monitor sports biomechanics with moderate to excellent accuracy. Therefore, this study also relies on the validation and repeated application of methods previously explored. Previous research primarily focused on the impact of individual gait variables when analyzing gait patterns. This study collected actual LCM data from subjects in both laboratory and outdoor settings, screened high-stress and low-stress feature data using multiple correlation coefficient methods, and demonstrated the potential to gather extensive clinical biomechanical data using portable wireless devices.

5. Conclusion

IMUs bridge the gap between laboratory and clinical biomechanical assessments, enabling the acquisition of objective human motion data in unconstrained environments at a low cost. This capability has led to further research and discussions. Combining machine learning and IMUs for classifying or predicting known datasets is currently a cost-effective and applicable method. Studies have demonstrated that IMU systems can monitor sports biomechanics with moderate to excellent accuracy. Therefore, this study also relies on the validation and repeated application of methods previously explored. Previous research primarily focused on the impact of individual gait variables when analyzing gait patterns. This study collected actual LCM data from subjects in both laboratory and outdoor settings, screened high-stress and low-stress feature data using multiple correlation coefficient methods, and demonstrated the potential to gather extensive clinical biomechanical data using portable wireless devices.

This study found that, compared to other LCM directions and running, the knee joint exhibited higher flexion angles, abduction moments, and increased knee contact forces in the frontal plane during 90° LCM. Calculations using OpenSim tools revealed that ACL strain values during 90° LCM were significantly higher than those during other movement states, particularly during the initial landing and push-off phases. By utilizing the random forest classification model, inertial sensor feature data were separately trained and validated. The results demonstrated that the model exhibited high sensitivity and accuracy (both exceeding 95%) for time-domain and frequency-domain features such as "kurtosis," "skewness," "variance," "energy," and the "25th percentile," offering valuable insight into the selection of input features for similar classification model training.

6. References

[1] Sheppard, J.M.; Young, W.B. Agility literature review: Classifications, training and testing. Journal of sports sciences 2006, 24, 919-932.

[2] Dos'Santos, T.; Thomas, C.; McBurnie, A.; Comfort, P.; Jones, P.A. Change of direction speed and technique modification training improves 180 turning performance, kinetics, and kinematics. Sports 2021, 9, 73.

[3] Jindrich, D.L.; Smith, N.C.; Jespers, K.; Wilson, A.M. Mechanics of cutting maneuvers by ostriches (Struthio camelus). Journal of Experimental Biology 2007, 210, 1378-1390.

[4] Havens, K.L.; Sigward, S.M. Whole body mechanics differ among running and cutting maneuvers in skilled athletes. Gait & posture 2015, 42, 240-245.

[5] Boden, B.P.; Dean, G.S.; Feagin, J.A.; Garrett, W.E. Mechanisms of anterior cruciate ligament injury. 2000, 23, 573-578.

[6] Chappell, J.D.; Herman, D.C.; Knight, B.S.; Kirkendall, D.T.; Garrett, W.E.; Yu, B. Effect of fatigue on knee kinetics and kinematics in stop-jump tasks. The American journal of sports medicine 2005, 33, 1022-1029.

[7] Besier, T.F.; Lloyd, D.G.; Ackland, T.R. Muscle activation strategies at the knee during running and cutting maneuvers. Medicine and science in sports and exercise 2003, 35, 119-127.

[8] Benjaminse, A.; Habu, A.; Sell, T.C.; Abt, J.P.; Fu, F.H.; Myers, J.B.; Lephart, S.M. Fatigue alters lower extremity kinematics during a single-leg stop-jump task. Knee Surgery, Sports Traumatology, Arthroscopy 2008, 16, 400-407.

[9] Padua, D.A.; Arnold, B.L.; Perrin, D.H.; Gansneder, B.M.; Carcia, C.R.; Granata, K.P. Fatigue, vertical leg stiffness, and stiffness control strategies in males and females. Journal of athletic training 2006, 41, 294.

[10] David, S.; Mundt, M.; Komnik, I.; Potthast, W. Understanding cutting maneuvers – The mechanical consequence of preparatory strategies and foot strike pattern. Human Movement Science 2018, 62, 202-210, doi:https://doi.org/10.1016/j.humov.2018.10.005.

[11] Patoz, A.; Lussiana, T.; Breine, B.; Gindre, C.; Malatesta, D. Both a single sacral marker and the whole-body center of mass accurately estimate peak vertical ground reaction force in running. Gait & Posture 2021, 89, 186-192.

[12] Verheul, J.; Nedergaard, N.J.; Vanrenterghem, J.; Robinson, M.A. Measuring biomechanical loads in team sports–from lab to field. Science and Medicine in Football 2020, 4, 246-252.

[13] van der Kruk, E.; Reijne, M.M. Accuracy of human motion capture systems for sport applications; state-of-the-art review. European journal of sport science 2018, 18, 806-819.

[14] Di Paolo, S.; Lopomo, N.F.; Della Villa, F.; Paolini, G.; Figari, G.; Bragonzoni, L.; Grassi, A.; Zaffagnini, S. Rehabilitation and return to sport assessment after anterior cruciate ligament injury: quantifying joint kinematics during complex high-speed tasks through wearable sensors. Sensors 2021, 21, 2331.

[15] Camomilla, V.; Bergamini, E.; Fantozzi, S.; Vannozzi, G. Trends Supporting the In-Field Use of Wearable Inertial Sensors for Sport Performance Evaluation: A Systematic Review. Sensors 2018, 18, 873.

[16] Jang, W.-J.; Lee, K.-K.; Lee, W.-J.; Lim, S.-H. Development of an Inertial Sensor Module for Categorizing Anomalous Kicks in Taekwondo and Monitoring the Level of Impact. Sensors 2022, 22, 2591.

[17] Han, S.-L.; Xie, M.-J.; Chien, C.-C.; Cheng, Y.-C.; Tsao, C.-W. Using MEMS-based inertial sensor with ankle foot orthosis for telerehabilitation and its clinical evaluation in brain injuries and total knee replacement patients. Microsystem Technologies 2016, 22,

625-634.

[18] Giggins, O.M.; Sweeney, K.T.; Caulfield, B. Rehabilitation exercise assessment using inertial sensors: a cross-sectional analytical study. Journal of neuroengineering and rehabilitation 2014, 11, 1-10.

[19] Delp, S.L.; Anderson, F.C.; Arnold, A.S.; Loan, P.; Habib, A.; John, C.T.; Guendelman, E.; Thelen, D.G. OpenSim: open-source software to create and analyze dynamic simulations of movement. IEEE transactions on biomedical engineering 2007, 54, 1940-1950.

[20] Tenforde, A.S.; Hayano, T.; Jamison, S.T.; Outerleys, J.; Davis, I.S. Tibial acceleration measured from wearable sensors is associated with loading rates in injured runners. PM&R 2020, 12, 679-684.

[21] Koga, H.; Muneta, T. ACL injury mechanisms. ACL injury and its treatment 2016, 113-125.

[22] Cheng, E.J.; Brown, I.E.; Loeb, G.E. Virtual muscle: a computational approach to understanding the effects of muscle properties on motor control. Journal of neuroscience methods 2000, 101, 117-130.

[23] Shorten, M.R.; Winslow, D.S. Spectral analysis of impact shock during running. Journal of Applied Biomechanics 1992, 8, 288-304.

[24] Hennig, E.M.; Lafortune, M.A. Relationships between ground reaction force and tibial bone acceleration parameters. Journal of Applied Biomechanics 1991, 7, 303-309.

[25] Sheerin, K.R.; Reid, D.; Besier, T.F. The measurement of tibial acceleration in runners—A review of the factors that can affect tibial acceleration during running and evidence-based guidelines for its use. Gait & Posture 2019, 67, 12-24.

[26] Milner, C.E.; Hawkins, J.L.; Aubol, K.G. Tibial Acceleration during Running Is Higher in Field Testing Than Indoor Testing. Medicine and Science in Sports and Exercise 2020, 52, 1361-1366.

[27] Breiman, L. Random forests. Machine learning 2001, 45, 5-32.

[28] Pataky, T.C.; Vanrenterghem, J.; Robinson, M.A. Zero-vs. one-dimensional, parametric vs. non-parametric, and confidence interval vs. hypothesis testing procedures in one-dimensional biomechanical trajectory analysis. Journal of biomechanics 2015, 48, 1277-1285.